



OPEN ACCESS

RESEARCH PAPER

# Gyrification abnormalities in presymptomatic *c9orf72* expansion carriers

Eduardo Caverzasi,<sup>1</sup> Giovanni Battistella,<sup>1</sup> Stephanie A Chu,<sup>2</sup> Howie Rosen,<sup>2</sup> Theodore P Zanto,<sup>1</sup> Anna Karydas,<sup>1</sup> Wendy Shwe,<sup>2</sup> Giovanni Coppola,<sup>3</sup> Daniel H Geschwind,<sup>4</sup> Rosa Rademakers,<sup>5</sup> Bruce L Miller,<sup>2,6</sup> Maria Luisa Gorno-Tempini,<sup>2</sup> Suzee E Lee<sup>1</sup>

► Additional material is published online only. To view please visit the journal online (<http://dx.doi.org/10.1136/jnnp-2018-320265>).

<sup>1</sup>Neurology, University of California, San Francisco, San Francisco, California, USA

<sup>2</sup>Neurology, Memory and Aging Center University of California, San Francisco, San Francisco, California, USA

<sup>3</sup>Neurology, UCLA, Los Angeles, California, USA

<sup>4</sup>Psychiatry and Neurology, UCLA Semel Institute for Neuroscience and Human Behavior, Los Angeles, California, USA

<sup>5</sup>Neuroscience, Mayo Clinic College of Medicine, Jacksonville, Florida, USA

<sup>6</sup>University of California, San Francisco, San Francisco, California, USA

## Correspondence to

Dr Eduardo Caverzasi, Neurology, University of California, San Francisco, San Francisco, California, USA; [eduardo.caverzasi@ucsf.edu](mailto:eduardo.caverzasi@ucsf.edu)

EC and GB contributed equally. MLG-T and SEL contributed equally.

Received 23 December 2018

Revised 4 March 2019

Accepted 3 April 2019

Published Online First 11 May 2019



© Author(s) (or their employer(s)) 2019. Re-use permitted under CC BY-NC. No commercial re-use. See rights and permissions. Published by BMJ.

**To cite:** Caverzasi E, Battistella G, Chu SA, et al. *J Neurol Neurosurg Psychiatry* 2019;**90**:1005–1010.

## ABSTRACT

**Objective** To investigate in-vivo cortical gyrification patterns measured by the local gyrification index (LGI) in presymptomatic *c9orf72* expansion carriers compared with healthy controls, and investigate relationships between LGI and cortical thickness, an established morphometric measure of neurodegeneration.

**Methods** We assessed cortical gyrification and thickness patterns in a cohort of 15 presymptomatic *c9orf72* expansion carriers (age  $43.7 \pm 10.2$  years, 9 females) compared with 67 (age  $42.4 \pm 12.4$  years, 36 females) age and sex matched healthy controls using the dedicated Freesurfer pipeline.

**Results** Compared with controls, presymptomatic carriers showed significantly lower LGI in left frontal and right parieto-occipital regions. Interestingly, those areas with abnormal gyrification in presymptomatic carriers showed no concomitant cortical thickness abnormality. Overall, for both presymptomatic carriers and healthy controls, gyrification and cortical thickness measures were not correlated, suggesting that gyrification captures a feature distinct from cortical thickness.

**Conclusions** Presymptomatic *c9orf72* expansion carriers show regions of abnormally low gyrification as early as their 30s, decades before expected symptom onset. Cortical gyrification represents a novel grey matter metric distinctive from grey matter thickness or volume and detects differences in presymptomatic carriers at an early age.

## INTRODUCTION

A hexanucleotide expansion in *c9orf72* (C9) is the most common genetic cause of familial and sporadic frontotemporal dementia (FTD) and amyotrophic lateral sclerosis (ALS).<sup>1–2</sup> Previous studies show that presymptomatic *c9orf72* expansion carriers (preSxC9) have deficits in grey matter volume, white matter integrity<sup>3–5</sup> and disruption of functional connectivity networks as soon as their early 30s, decades before expected symptom onset.<sup>4</sup> These abnormalities may represent incipient neurodegeneration, abnormal brain development or both. Whether such deficits represent neurodevelopmental differences vs early atrophy, however, remains an open question.

Brain development is an intricate and complex process that begins during gestation and continues through early adulthood. Cortical folding, or

gyrification, represents a dynamic phenomenon allowing for abundant expansion of the cortical surface.<sup>6,7</sup> During the third trimester of fetal life, gyrification proliferates rapidly, and the brain grows from a relatively smooth surface towards a gyrification pattern resembling the adult brain.<sup>8–9</sup> Gyrification declines exponentially throughout childhood and adolescence, and then declines more linearly during adulthood, and these declines in gyrification arise in parallel with age-related volume loss.<sup>7,10</sup> With novel morphometric MRI techniques, three-dimensional cortical folding patterns can be evaluated in-vivo by computing the local gyrification index (LGI), defined as the ratio between the cortex buried within sulcal folds and the area of the cortical surface.<sup>11</sup>

In children with neurodevelopmental disorders such as dyslexia and autism, specific brain regions show a higher degree of cortical folding compared with typically developing children.<sup>12–15</sup> In dyslexia, this abnormally higher gyrification may be due to the absence of the age-related gyrification decline seen in typically developing children. Studies in adults have revealed abnormal gyrification trajectories in patients with major psychiatric disorders (ie, depression, bipolar disorder and schizophrenia)<sup>10</sup> and neurodegenerative disorders such as Parkinson's and Alzheimer's diseases.<sup>16–17</sup> In contrast to the pattern seen in neurodevelopmental disorders, patients with Alzheimer's disease show abnormally low gyrification associated with sulcal widening, reduced cortical thickness and cognitive decline.<sup>16</sup>

To date, no study has applied this novel metric to assess gyrification in presymptomatic carriers of any neurodegenerative disease-causing mutations. We hypothesised that presymptomatic *c9orf72* expansion carriers would have abnormally increased cortical gyrification as seen in dyslexia and autism, reflecting neurodevelopmental differences. In the present study, we assessed cortical gyrification and cortical thickness in 15 preSxC9 compared with age and sex matched healthy controls (HC).

## METHODS

### Subjects

We compared 15 preSxC9 (age  $43.7 \pm 10.2$  years, 9 females) to 67 (age  $42.4 \pm 12.4$  years, 36 females) age and sex matched HC. Demographic characteristics and neuropsychological test scores did not statistically differ between groups and are reported

## Neurodegeneration

in a previous study.<sup>4</sup> In genetic FTD, mean familial age of onset correlates with age of symptom onset in symptomatic carriers.<sup>5</sup> Thus, the estimated time to symptom onset for a presymptomatic carrier was calculated by determining the difference between the carrier's age and the mean familial age of onset. The estimated time to symptom onset of the presymptomatic carriers in the present study was  $8.2 \pm 11.0$  years. The University of California, San Francisco Committee on Human Research approved the study. Participants provided informed consent prior to participation.

### Image acquisition

All subjects underwent MRI scanning on a Siemens Tim Trio 3T scanner. Structural volumetric T1-weighted imaging was acquired with the following parameters: TR/TE 2300/2.98 ms; flip angle 9°; 160 sagittal slices; voxel size = 1 mm<sup>3</sup>; matrix size 240 x 256.<sup>4</sup>

### FreeSurfer-based cortical thickness and IGI analyses

The preprocessing of T1-weighted images was performed using FreeSurfer V5.3 (<http://surfer.nmr.mgh.harvard.edu/>) in accordance with a standard autoreconstruction algorithm. The pipeline included intensity normalisation, removal of non-brain tissue using a watershed algorithm technique, generation of the surface mesh representations using a surface deformation algorithm, tessellation of the grey matter boundary, automated topology correction and Talairach-Tournoux transformation.<sup>18–20</sup> The accuracy of the segmentation results was validated by a neuroradiologist (EC). Cortical thickness measures were obtained based on the shortest distance between the grey matter/white matter and grey matter/cerebrospinal fluid boundaries at each vertex of the tessellated surface. Gyrfication of the entire cortex was also assessed using FreeSurfer. IGI was computed using the method described by Schaer and colleagues.<sup>11, 21</sup> Cortical thickness and IGI images were normalised to the *fsaverage* space (MNI305 template) and smoothed with a full-width at half maximum Gaussian kernel of 15 mm for cortical thickness and 5 mm for IGI (figure 1).<sup>7</sup>

### Statistical analysis with AFNI

We examined group differences (preSxC9 vs HC) in cortical thickness and IGI using independent two-sample t-tests (AFNI 3dttest++, [www.afni.nimh.nih.gov](http://www.afni.nimh.nih.gov)) at two thresholds:  $p < 0.001$  uncorrected and  $p < 0.05$  corrected for family-wise error (FWE). We performed the FWE multiple comparison correction using the 'slow\_surf\_clustsim.py' and 'quick.alpha.vals.py' tools in the AFNI software package. We chose to report results at  $p < 0.001$

uncorrected, consistent with the previous study.<sup>4</sup> These t-tests perform a vertex-by-vertex regression over the whole cortical surface to estimate the mean difference of the input data between the two groups. Participants' age, gender and cortical thickness (for the IGI comparison) were included as covariates of no interest.<sup>22</sup> To explore potential differences between groups with respect to age, we examined group as an interaction term for the relationship between IGI and age. We also computed the effect size measured by Cohen's d (d) for each cluster found to have significantly lower IGI in the presymptomatic carriers; this was obtained by dividing the difference between mean values by the common SD of the two groups.<sup>23</sup> With the effect size, we performed a power calculation for a two-tailed analysis using an alpha value of 0.05.

### Relationship between cortical thickness and IGI

We performed a Pearson correlation analysis across the grey matter in all subjects to assess for potential associations between cortical thickness and IGI. We also performed a least squares regression (LSR) analysis to quantify the variance attributable to group, age or cortical thickness within the map of regions in which preSxC9 showed significantly abnormal IGI compared with HC. We used the JMP PRO 14 statistical programme to perform this analysis.

## RESULTS

### PreSxC9 show regions of lower gyrfication compared to healthy controls

PreSxC9 showed four regions of lower IGI compared with controls ( $p_{FWE} < 0.05$ ) in the left subgenual anterior cingulate cortex, left precentral gyrus, right inferior parietal lobule and right superior occipital gyrus (figure 2 and table 1). The effect size measured by Cohen's d was large ( $d = 1.0$ ) in each significant cluster with a power of 93.3%. A trend ( $p < 0.001$  uncorrected) towards lower IGI emerged in the left orbitofrontal, insular and occipital cortices and right parietal cortex (figure 2 and table 1). There were no regions for which preSxC9 had a significantly greater IGI compared with controls.

We next explored whether carriers and controls might have different cross-sectional relationships between gyrfication and increasing age. Across the entire cortical surface, there were no statistically significant regions for which the slope of IGI vs age differed between carriers and controls at either threshold. Within those regions showing lower IGI for preSxC9, both groups showed IGI declines with age, and the slopes of these

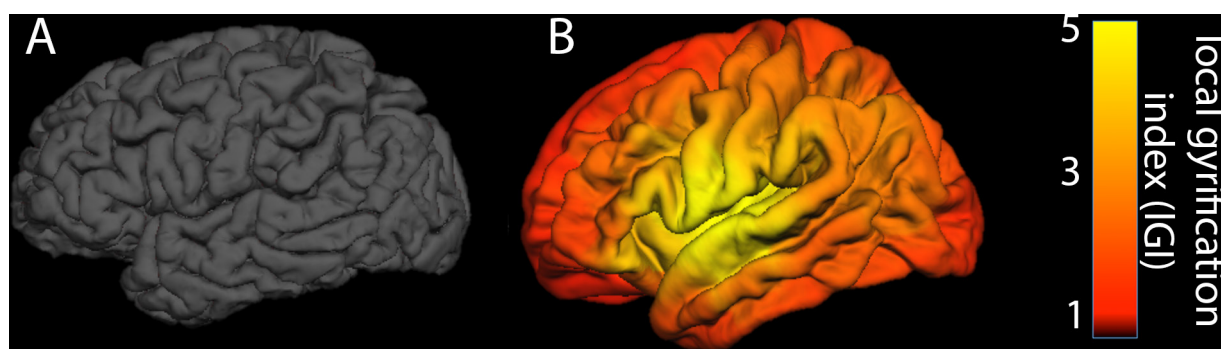


**Figure 1** Example of an individual subject IGI map. (A) Lateral view of the native space cortical surface of one healthy control subject (male, 57 years old) and (B) lateral view of the IGI map overlaid on the FreeSurfer *fsaverage* template. Regions with a higher IGI indicate a greater degree of gyrfication. The 'heat' colour bar represents IGI values, ranging from 0 to 5. IGI, local gyrfication index.

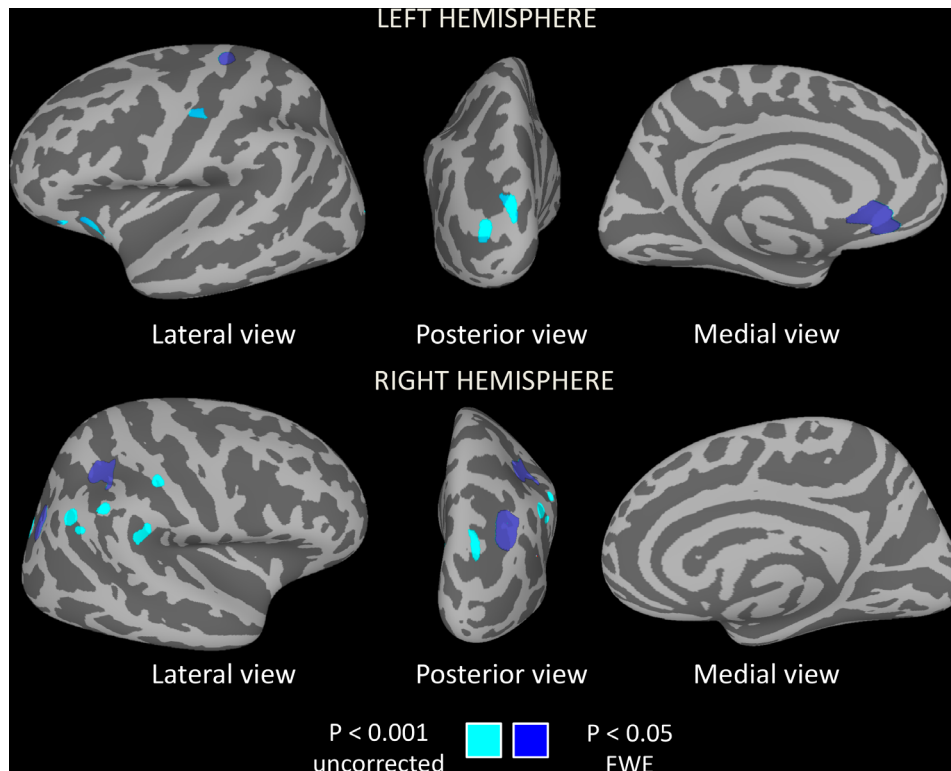


**Figure 2** PreSxC9 show regions with low local gyrification index. Regions with significantly lower local gyrification index emerged in preSxC9 compared with controls ( $p < 0.001$  uncorrected, cyan). Regions in left precentral gyrus, left subgenual anterior cingulate, right superior occipital cortex and right inferior parietal lobule remained significant at  $p_{FWE} < 0.05$  (dark blue). FWE, family-wise error.

IGI declines with age did not significantly differ between groups (figure 3).

Compared with controls, preSxC9 did not show any differences in cortical thickness at  $p_{FWE} < 0.05$ . Regions of lower cortical thickness in preSxC9 emerged at  $p < 0.001$  uncorrected in frontal, insular, cingulate and occipital cortex bilaterally (online supplementary data). There were no regions for which

preSxC9 had a significantly greater cortical thickness compared with controls at  $p < 0.001$  uncorrected.

### Gyrification and cortical thickness are uncorrelated

To probe whether IGI represents a metric independent from cortical thickness, we correlated cortical thickness and IGI for the entire grey matter across all subjects. There was no significant correlation between cortical thickness and IGI at  $p_{FWE} < 0.05$ . We next correlated IGI and thickness within each subject subgroup, and no correlations emerged at either threshold for the preSxC9 or the HC groups. Overall, these analyses suggest that IGI and thickness capture independent characteristics of grey matter within our study cohort.

To quantify the relative contributions of group, cortical thickness, age and sex to the variance of IGI, we performed an LSR analysis for regions in the preSxC9 < HC IGI map ( $p_{FWE} < 0.05$ ). The model that best explained IGI variability ( $R^2 = 0.37$ ;  $p < 0.0001$ ) included group ( $\beta = -5.30$ ;  $p < 0.0001$ ) and age ( $\beta = -3.26$ ;  $p = 0.002$ ). As expected, the variance within regions of low gyrification in preSxC9 was most strongly attributable to group, then age. Interestingly, cortical thickness and sex were not predictors of IGI.

### DISCUSSION

PreSxC9 feature structural brain deficits decades before expected symptom onset, with grey and white matter declines with age at a rate similar to controls,<sup>4</sup> leading to the intriguing hypothesis that such deficits may represent neurodevelopmental differences. Because neurodevelopmental disorders such as dyslexia and autism feature regions of abnormally increased gyrification, we had hypothesised that preSxC9 would also show cortical regions of 'hypergyrification'. In contrast to our hypothesis, we found

**Table 1** Regions showing lower local gyrification in preSxC9

Local gyrification index						
	Cluster	Area	T value	MNI x	MNI y	MNI z
Left-sided	<b>Subgenual anterior cingulate (L) *</b>	218.06	3.60	-3.79	29.66	-9.49
	<b>Precentral (F) *</b>	174.37	3.69	-28.21	-24.61	62.59
	Middle occipital (O)	79.59	3.65	-27.88	-95.34	11.38
	Sup occipital (O)	77.58	3.55	-13.86	-95.89	19.84
	Orbito frontal (F)	57.51	3.52	-23.14	11.71	-24.32
	Ant insula (L)	56.01	3.58	-29.87	22.84	-7.97
	Central sulcus (F-P)	40.34	3.49	-42.39	-15.12	33.48
	Orbito frontal (F)	27.44	3.55	-41.35	27.92	-16.78
Right-sided	<b>Sup occipital (O) *</b>	273.91	3.76	32.38	-73.12	30.84
	<b>Inferior parietal (P) *</b>	142.50	3.54	34.03	-40.30	41.84
	Sup occipital (O)	109.24	3.55	25.83	-83.94	25.06
	Supramarginal (P)	73.04	3.62	52.27	-33.96	28.92
	Angular (P)	67.80	3.59	50.63	-57.94	39.87
	Postcentral (P)	55.01	3.52	54.09	-19.81	45.29
	Supramarginal (P)	51.11	3.55	54.30	-44.70	43.17
	Sup temporal (T)	28.93	3.45	51.19	-54.91	31.49

The table lists all clusters showing regions of reduced local gyrification index in preSxC9 ( $p < 0.001$  uncorrected). Regions in bold font and marked with "\*" remained significant after family-wise error correction. We also indicate the brain region to which each cluster belongs: frontal (F), temporal (T), parietal (P), occipital (O) or limbic (L). Clusters' coordinates are listed in MNI305 space (fsaverage brain of FreeSurfer).

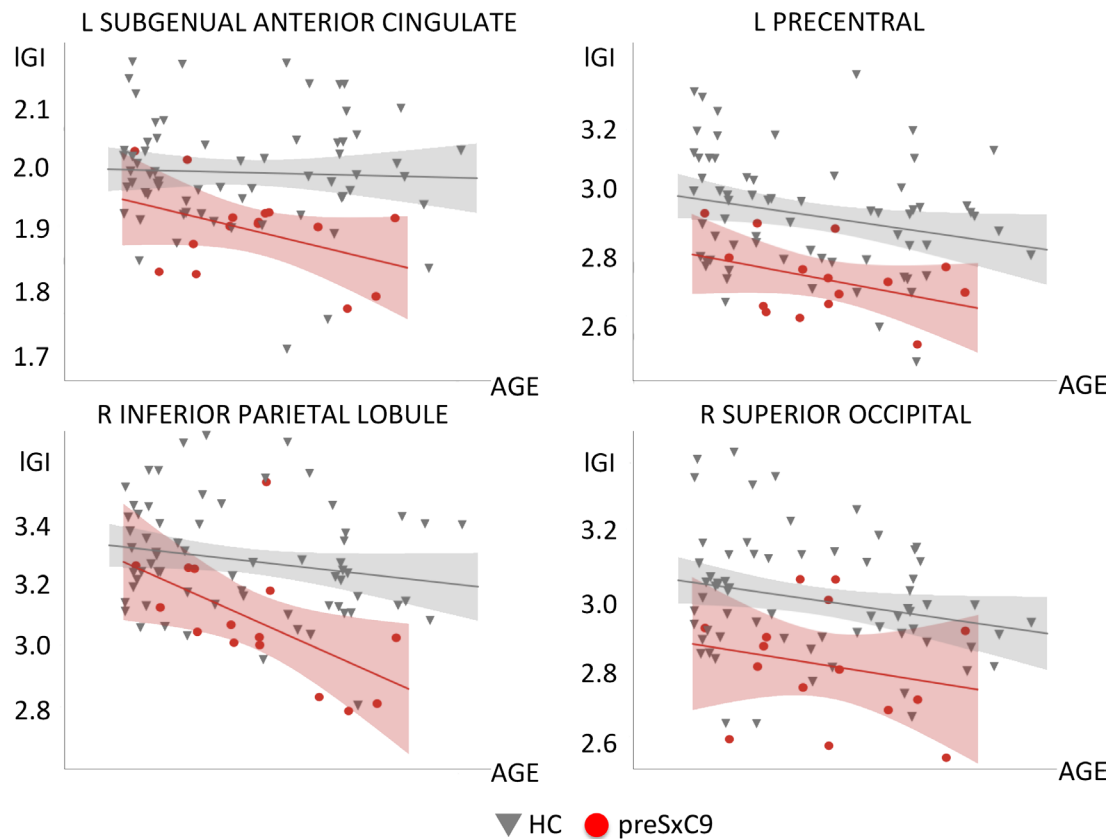


**Figure 3** Relationships with age for regions showing low IGI. We extracted the mean IGI within each of the four regions showing low IGI in preSxC9 compared with HC (at  $p$ FWE <0.05). These clusters appeared within left precentral gyrus, left subgenual anterior cingulate, right superior occipital gyrus and right inferior parietal lobule. HC (dark grey), preSxC9 (red) fit lines are shown for visualisation purposes only. Age axis labels are removed to protect participant anonymity. FWE, family-wise error; HC, healthy controls; IGI, local gyrification index.

that preSxC9 had no regions of increased gyrification, but instead regions of low IGI in the left subgenual anterior cingulate cortex, left precentral gyrus, right inferior parietal lobule and right superior occipital gyrus. Both preSxC9 and controls showed decreasing IGI across the adult age span studied, without any difference in slopes for the relationship between IGI and age. Low IGI values appeared in carriers as young as their 30s, consistent with previous findings that preSxC9 have grey matter deficits at this age.<sup>4</sup> Interestingly, regions of low gyrification in preSxC9 only partially overlapped with regions of low grey matter thickness and volume, and within regions of low gyrification, cortical thickness was not a significant predictor of IGI variance. Moreover, gyrification and thickness were uncorrelated across the entire cortex. These findings support the notion that gyrification captures a feature of the cortex that is distinctive from grey matter thickness or volume and that gyrification may prove a useful marker for detecting differences in presymptomatic carriers.

### PreSxC9 have low gyrification in regions atrophied during the symptomatic phase

As with sporadic bvFTD, patients with bvFTD due to the *c9orf72* expansion show symmetric, prominent atrophy in the anterior insula, anterior cingulate and frontotemporal cortex.<sup>24–27</sup> In contrast to sporadic bvFTD, *c9orf72*-bvFTD features parietal, occipital<sup>26,27</sup> and thalamic atrophy.<sup>28</sup> Similarly, patients with ALS due to the *c9orf72* expansion show a more distributed atrophy pattern, with a greater degree of frontal and anterior cingulate atrophy<sup>29</sup> and thalamic degeneration<sup>30</sup> compared with sporadic ALS. PreSxC9 show grey matter deficits in regions that atrophy in *c9orf72*-bvFTD, including

the anterior cingulate, medial frontal and dorsolateral prefrontal cortex, insula, precentral gyrus, precuneus, occipital cortex, striatum and medial thalamus.<sup>4</sup>

The regions with low gyrification in preSxC9 are congruent with regions of grey matter atrophy in *c9orf72*-bvFTD<sup>28</sup> and grey matter volume deficits in preSxC9.<sup>4</sup> PreSxC9 showed low IGI in the anterior cingulate cortex, which represents a key region of atrophy in bvFTD with or without *c9orf72*.<sup>28,31</sup> The low IGI found in the primary motor cortex in presymptomatic carriers may presage future vulnerability to motor neuron disease that manifests during the symptomatic phase. Regions of low IGI also emerged in parieto-occipital cortex, consistent with grey matter atrophy and deficits in *c9orf72*-bvFTD and presymptomatic carriers.<sup>4,28</sup>

### Low gyrification in preSxC9: neurodevelopmental versus neurodegenerative?

Whether regions of low gyrification in preSxC9 represent a neurodevelopmental difference or early atrophy remains an open question. We identified regions of low gyrification in carriers as young as their 30s, presumably decades before expected symptom onset. This finding is parallel to a previous study in which these same presymptomatic carriers showed grey matter volume and white matter deficits at a similar age.<sup>4</sup> In the present study and the previous study, both IGI and grey and white matter declined with age in preSxC9 at rate similar to controls, suggesting that these deficits may be due to neurodevelopmental differences.

Previous studies have revealed that children with dyslexia and autism show regions of abnormally high IGI. In dyslexia,

regions with abnormally increased IGI correlate with neurite morphology, possibly associated with synaptic pruning deficits.<sup>15</sup> In contrast to these developmental disorders in children, preSxC9 showed low IGI compared with controls. One possibility is that low gyrification represents a developmental deficit in cortical expansion in preSxC9, resulting in low IGI throughout the entire lifespan. A second possibility is that low IGI values could reflect that preSxC9 subjects ‘overprune’ gyri during adolescence and early adulthood to a degree beyond the typical decline in gyrification seen during adulthood. If due to developmental differences, these regions with low IGI may represent vulnerable regions that set the path for focal future neurodegeneration. A third consideration is that low IGI could represent early atrophy in preSxC9. PreSxC9 show gyrification declines with age at a rate similar to controls. If low IGI were to represent atrophy, however, we would expect to see accelerated IGI decline as seen in Alzheimer’s and Parkinson’s diseases,<sup>16 17</sup> yet our cross-sectional data did not show an accelerated decline in IGI for older carriers. Future longitudinal studies, including those with children and adolescents, are needed to establish trajectories of IGI and other imaging metrics to determine the natural history of brain development.

### Relationships between gyrification and other imaging measures

Our data suggest that the regions of low gyrification in preSxC9 were not attributable to cortical thickness deficits, consistent with other studies that have examined the relationship between IGI and other grey matter metrics. In a study of typically developing children and healthy adults, IGI correlated with grey matter volume but not with cortical thickness.<sup>7</sup> In parallel, a study of adolescents with autism also showed that IGI and cortical thickness were uncorrelated, and that instead, IGI correlates with white matter architecture and connectivity.<sup>32</sup>

Previous studies suggest that gyrification has stronger associations with structural white matter connectivity rather than cortical thickness. In dyslexia, abnormally increased gyrification is correlated with neurite architecture changes as measured by neurite orientation dispersion and density imaging<sup>15</sup>; in autism spectrum disorder, increased gyrification is associated with altered white matter organisation.<sup>12</sup> Although the mechanics of gyrification remain opaque, one theory suggests that cortical folding is driven to optimise white matter connections, as tension-mediated forces along axons bring highly connected regions closer to each other.<sup>6</sup> In support of this theory, the immense increase in brain gyrification during the late fetal period coincides with an explosive development of cortico-cortical connections.<sup>6 15 33–36</sup> Future studies will inform the relationships between white matter structural connectivity and gyrification in preSxC9 and other neurodevelopmental disorders.

### CONCLUSIONS

PreSxC9 show regions of abnormally low gyrification in regions known to be targeted in *c9orf72*-FTD and *c9orf72*-ALS. If neurodevelopmental, deficits in gyrification and grey matter volume may confer vulnerability that predisposes selective brain regions to future neurodegeneration. Cortical gyrification represents a novel grey matter metric, and future longitudinal studies will clarify if low gyrification in preSxC9 represents a neurodevelopmental phenomenon.

**Acknowledgements** We thank all participants and their families whose help and participation made this work possible.

**Contributors** EC and GB designed and conceptualised the study. They processed the data, performed the statistical analysis of the data and drafted the manuscript for intellectual content. SAC, AMK and WS were involved in the data collection. HLR, TPZ, GC, DHG and RR were involved in the data collection and revision of the manuscript for intellectual content. BLM revised the manuscript for intellectual content. MLG-T and SEL were involved in the design and conceptualisation of the study and revision of the manuscript for intellectual content.

**Funding** This work was supported by the National Institutes of Health [SEL: R01 AG058233, K23AG039414; TPZ: F32AG030249, R01MH096861; MGT: R01NS050915, K24DC015544; GC: AG035610; RR: R35NS097261; BLM: P01AG019724, P50AG23501]. The John Douglas French Alzheimer’s Foundation [GC]. State of California DHS04-35516 [MGT]. Samples from the National Cell Repository for Alzheimer’s Disease (NCRAD), which receives government support under a cooperative agreement grant (U24AG21886) awarded by the National Institute on Aging (NIA), were used in this study.

**Competing interests** None declared.

**Patient consent for publication** Not required.

**Provenance and peer review** Not commissioned; externally peer reviewed.

**Data availability statement** Researchers may obtain imaging code used for preprocessing and statistical analysis in this study from the corresponding author on reasonable request. All data relevant to the study are included in the article or uploaded as supplementary information.

**Open access** This is an open access article distributed in accordance with the Creative Commons Attribution Non Commercial (CC BY-NC 4.0) license, which permits others to distribute, remix, adapt, build upon this work non-commercially, and license their derivative works on different terms, provided the original work is properly cited, appropriate credit is given, any changes made indicated, and the use is non-commercial. See: <http://creativecommons.org/licenses/by-nc/4.0/>.

### REFERENCES

- DeJesus-Hernandez M, Mackenzie IR, Boeve BF, *et al.* Expanded GGGGCC hexanucleotide repeat in noncoding region of *C9orf72* causes chromosome 9p-linked FTD and ALS. *Neuron* 2011;72:245–56.
- Renton AE, Majounie E, Waite A, *et al.* A hexanucleotide repeat expansion in *C9orf72* is the cause of chromosome 9p21-linked ALS-FTD. *Neuron* 2011;72:257–68.
- Bertrand A, Wen J, Rinaldi D, *et al.* Early cognitive, structural, and microstructural changes in presymptomatic *C9orf72* carriers younger than 40 years. *JAMA Neurol* 2018;75:236–45.
- Lee SE, Sias AC, Mandelli ML, *et al.* Network degeneration and dysfunction in presymptomatic *C9orf72* expansion carriers. *Neuroimage Clin* 2017;14:286–97.
- Rohrer JD, Nicholas JM, Cash DM, *et al.* Presymptomatic cognitive and neuroanatomical changes in genetic frontotemporal dementia in the genetic frontotemporal dementia Initiative (GENFI) study: a cross-sectional analysis. *Lancet Neurol* 2015;14:253–62.
- White T, Su S, Schmidt M, *et al.* The development of gyrification in childhood and adolescence. *Brain Cogn* 2010;72:36–45.
- Klein D, Rotarska-Jagiela A, Genc E, *et al.* Adolescent brain maturation and cortical folding: evidence for reductions in gyrification. *PLoS One* 2014;9:e84914.
- Armstrong E, Schleicher A, Omran H, *et al.* The ontogeny of human gyrification. *Cereb Cortex* 1995;5:56–63.
- Zilles K, Palomero-Gallagher N, Amunts K. Development of cortical folding during evolution and ontogeny. *Trends Neurosci* 2013;36:275–84.
- Cao B, Mwangi B, Passos IC, *et al.* Lifespan gyrification trajectories of human brain in healthy individuals and patients with major psychiatric disorders. *Sci Rep* 2017;7.
- Schaer M, Cuadra MB, Schmansky N, *et al.* How to measure cortical folding from MR images: A step-by-step tutorial to compute local gyrification index. *J Vis Exp* 2012;(59).
- Ecker C, Andrews D, Dell’Acqua F, *et al.* Relationship between cortical gyrification, white matter connectivity, and autism spectrum disorder. *Cereb Cortex* 2016;26:3297–309.
- Mous SE, Karatekin C, Kao C-Y, *et al.* Gyrification differences in children and adolescents with velocardiofacial syndrome and attention-deficit/hyperactivity disorder: a pilot study. *Psychiatry Res* 2014;221:169–71.
- Fairchild G, Toschi N, Hagan CC, *et al.* Cortical thickness, surface area, and folding alterations in male youths with conduct disorder and varying levels of callous-unemotional traits. *Neuroimage Clin* 2015;8:253–60.
- Caverzasi E, Mandelli ML, Hoeft F, *et al.* Abnormal age-related cortical folding and neurite morphology in children with developmental dyslexia. *Neuroimage Clin* 2018;18:814–21.
- Liu T, Lipnicki DM, Zhu W, *et al.* Cortical gyrification and sulcal spans in early stage Alzheimer’s disease. *PLoS One* 2012;7:e31083.
- Zhang Y, Zhang J, Xu J, *et al.* Cortical gyrification reductions and subcortical atrophy in Parkinson’s disease. *Mov Disord* 2014;29:122–6.

- 18 Dale AM, Fischl B, Sereno MI. Cortical surface-based analysis. I. segmentation and surface reconstruction. *Neuroimage* 1999;9:179–94.
- 19 Fischl B, Sereno MI, Dale AM. Cortical surface-based analysis. II: inflation, flattening, and a surface-based coordinate system. *Neuroimage* 1999;9:195–207.
- 20 Fischl B, Sereno MI, Tootell RB, et al. High-resolution intersubject averaging and a coordinate system for the cortical surface. *Hum Brain Mapp* 1999;8:272–84.
- 21 Schaer M, Cuadra MB, Tamarit L, et al. A surface-based approach to quantify local cortical gyrification. *IEEE Trans Med Imaging* 2008;27:161–70.
- 22 Bianchi S, Battistella G, Huddleston H, et al. Phenotype- and genotype-specific structural alterations in spasmodic dysphonia. *Mov Disord* 2017;32:560–8.
- 23 Cohen JA. *Statistical Power Analysis for the Behavioral Sciences*. Hillsdale, NJ, USA: Lawrence Erlbaum Associates, 1988.
- 24 Boxer AL, Mackenzie IR, Boeve BF, et al. Clinical, neuroimaging and neuropathological features of a new chromosome 9p-linked FTD-ALS family. *J Neurol Neurosurg Psychiatry* 2011;82:196–203.
- 25 Mahoney CJ, Beck J, Rohrer JD, et al. Frontotemporal dementia with the C9orf72 hexanucleotide repeat expansion: clinical, neuroanatomical and neuropathological features. *Brain* 2012;135:736–50.
- 26 Sha SJ, Takada LT, Rankin KP, et al. Frontotemporal dementia due to C9ORF72 mutations: clinical and imaging features. *Neurology* 2012;79:1002–11.
- 27 Whitwell JL, Weigand SD, Boeve BF, et al. Neuroimaging signatures of frontotemporal dementia genetics: C9orf72, tau, progranulin and sporadics. *Brain* 2012;135:794–806.
- 28 Lee SE, Khazenon AM, Trujillo AJ, et al. Altered network connectivity in frontotemporal dementia with C9orf72 hexanucleotide repeat expansion. *Brain* 2014;137:3047–60.
- 29 Byrne S, Elamin M, Bede P, et al. Cognitive and clinical characteristics of patients with amyotrophic lateral sclerosis carrying a C9orf72 repeat expansion: a population-based cohort study. *Lancet Neurol* 2012;11:232–40.
- 30 Bede P, Bokde ALW, Byrne S, et al. Multiparametric MRI study of ALS stratified for the C9orf72 genotype. *Neurology* 2013;81:361–9.
- 31 Seeley WW, Crawford R, Rascovsky K, et al. Frontal paralimbic network atrophy in very mild behavioral variant frontotemporal dementia. *Arch Neurol* 2008;65:249–55.
- 32 Wallace GL, Robustelli B, Dankner N, et al. Increased gyrification, but comparable surface area in adolescents with autism spectrum disorders. *Brain* 2013;136:1956–67.
- 33 Van Essen DC. A tension-based theory of morphogenesis and compact wiring in the central nervous system. *Nature* 1997;385:313–8.
- 34 Takahashi E, Folkerth RD, Galaburda AM, et al. Emerging cerebral connectivity in the human fetal brain: an Mr tractography study. *Cereb Cortex* 2012;22:455–64.
- 35 Mitter C, Prayer D, Brugger PC, et al. In vivo tractography of fetal association fibers. *PLoS One* 2015;10:e0119536.
- 36 Vasung L, Lepage C, Radoš M, et al. Quantitative and qualitative analysis of transient fetal compartments during prenatal human brain development. *Front Neuroanat* 2016;10.